Biochemistry and Biophysics Reports 38 (2024) 101690

Contents lists available at ScienceDirect

Biochemistry and Biophysics Reports

journal homepage: www.elsevier.com/locate/bbrep

Glioblastoma U-87 cell electrotaxis is hindered by doxycycline with a concomitant reduction in the matrix metallopeptidase-9 expression

Hui-Fang Chang [a], Ji-Yen Cheng [a,b,c,d,*]

[a] Research Center for Applied Sciences, Academia Sinica, Taipei, Taiwan
[b] Institute of Biophotonics, National Yang Ming Chiao Tung University, Taipei, Taiwan
[c] Department of Mechanical and Mechatronic Engineering, National Taiwan Ocean University, Keelung, Taiwan
[d] College of Engineering, Chang Gung University, Taoyuan, Taiwan

ARTICLE INFO

Keywords:
Doxycycline
Electrotaxis
Microfluidic
Cancer metastasis
Glioblastoma cell
MMP-9

ABSTRACT

Electric fields (EF) play an essential role in cancer cell migration. Numerous cancer cell types exhibit electrotaxis under direct current electric fields (dcEF) of physiological electric field strength (EFs). This study investigated the effects of doxycycline on the electrotactic responses of U87 cells. After EF stimulation, U87 cells migrated toward the cathode, whereas doxycycline-treated U87 cells exhibited enhanced cell mobility but hindered cathodal migration. We further investigated the expression of the metastasis-correlated proteins matrix metallopeptidase-2 (MMP-2) and MMP-9 in U87 cells. The levels of MMP-2 in the cells were not altered under EF or doxycycline stimulation. In contrast, the EF stimulation greatly enhanced the levels of MMP-9 and then repressed in doxycycline-cotreated cells, accompanied by reduced cathodal migration. Our results demonstrated that an antibiotic at a non-toxic concentration could suppress the enhanced cell migration accelerated by EF of physiological strength. This finding may be applied as an anti-metastatic treatment for cancers.

1. Introduction

Electrotaxis is the directional migration of adherent cells in response to an electric field (EF) [1,2]. Previous studies have reported that EF plays crucial physiological roles, such as cell division [3], differentiation [4], migration [5–8], and death [9]. Several studies have shown that A549 (human lung adenocarcinoma cell line), H1650-M3 (non-small cell lung cancer, NSCLC), HeLa (human cervical cancer cell line), HeLa Tet-Off (tetracycline-off), HSC-3 (human oral squamous carcinoma cell line), HT-1080 (human sarcoma cell line), MCF-7 (human breast cancer cell line), NCI–H460 (human large cell lung carcinoma cell line), NCI–H520 (human lung squamous cell carcinoma), NCI–H1975 (human lung adenocarcinoma), and U-251 MG (human glioblastoma astrocytoma) cells migrate toward the cathode; whereas CL1-5 (human lung cancer cell line), DAOY (human medulloblastoma cell line), HCC827 (human lung adenocarcinoma cell line), NCI–H1299 (human lung cancer cell line), MDA-MB-231 (human breast cancer cell line), PC-3-M (human prostate cancer cell line), SaOS-2 (human osteosarcoma cell line), and T98G (human glioblastoma cell line) cells migrate toward the anode under EF stimulation [1,10–27]. These reports have indicated that EF functions as a key guiding cue and triggers the directional migration of cancer cells. Since endogenous EF has been observed across epithelium and endothelium [28–30], the effect of physiological EF on cancer cell migration requires scrutinization.

Cancer metastasis is the primary cause of cancer morbidity and mortality; most deaths (at least 2/3) caused by solid tumors are attributed to metastases [31]. Cancer cell migration and invasion are the initial steps of metastasis [32]. According to the World Health Organization classification system, glioblastoma, the most common brain malignancy, is a highly aggressive brain tumor belonging to grade IV gliomas [33]. It is thus important to investigate the effect of external stimulations on cell migration using a glioblastoma cell line. U87 cells are one of the most widely used glioblastoma model cells and are therefore chosen in the present study. Previous studies have shown that EF induces the biological response of U87 cells. In the work reported by Carr et al. nanosecond pulsed electric fields (nsPEF) disrupted the microtubule network and the microtubule growth dynamics [34]. In the work performed by Soueidet et al. U87 cells kept the mitochondrial potential and lost the plasma membrane integrity after nsPEF stimulation [35]. Moreover, Petrov et al. reported that the pulsed EF causes a change in mitochondrial activity in U87 cells [36]. These reports have revealed that EF can affect the biological responses of U87 cells.

* Corresponding author. Research Center for Applied Sciences, Academia Sinica, No. 128, Sec. 2, Academia Rd., Nangang Dist., Taipei City, 115201, Taiwan.
E-mail address: jycheng@gate.sinica.edu.tw (J.-Y. Cheng).

https://doi.org/10.1016/j.bbrep.2024.101690
Received 18 September 2023; Received in revised form 15 March 2024; Accepted 19 March 2024

Compared with normal brain tissue, matrix metalloproteinase-2 (MMP-2) and MMP-9 are highly expressed in glioblastomas. MMP-2 and MMP-9 regulate cellular proliferation, motility, invasion, and angiogenesis of glioblastomas. In addition, the upregulation of MMP-2 and MMP-9 in tumor cells is correlated with an increased glioblastoma malignancy grade [37–41].

Doxycycline is an antibiotic that is used to treat infections [42,43] and as a potential anti-cancer agent against human breast cancer cells [44], human osteosarcoma cells [45], and prostate cancer cells [46]. Moreover, doxycycline may help treat osteoblastic bone metastasis [47], inhibit metastasis in prostate cancer [48], and suppress NCI–H446 lung cancer cell metastasis [49]. To our knowledge, there has been rare report regarding the effect of doxycycline on the metastasis of glioblastoma. Thus, it is critical to understand the effect of doxycycline treatment on U-87 MG (U87) cells to identify efficient therapeutic strategies.

Previously, we have observed that doxycycline diminishes the electrotaxis of non-small cell lung cancer cells [26]. Since the combined effect of EF and doxycycline on U87 cells has rarely been reported, we investigated the EF-induced migration of U87 cells in the present work. We explored the effect of doxycycline on U87 cell electrotaxis and evaluated whether EF enhances the levels of peptidases, MMP-2 and MMP-9, in U87 cells. Furthermore, the effect of doxycycline on the EF-effected peptidase changes was examined.

2. Materials and methods

2.1. Electrotaxis chip design and fabrication

A home-developed electrotaxis chip modified from our previous works was used to study U87 cell electrotaxis. The chip design and detailed fabrication procedure were described in the previous works [1,17,50–52]. The chip configuration for electrotaxis is shown in Fig. 1A. The three PMMA sheets and the double-sided tape were patterned by cutting using a CO_2 laser scriber—the three channels (Channel 1 to Channel 3) form contamination-free regions for the cells therein. The patterns on these layers were drawn using the AutoCAD package and sent to the scriber for the cutting. All components of the layers were disinfected via exposure to UV light for 30 min before the chip assembly. The adaptors (the red, blue, and green cubes) adhered to the chip and provided the leakage-free connection to medium (red and green adaptors) and agarose bridges (blue adaptors) through finger-tightened fluidic fittings [52]. Then, the assembled electrotaxis chip (Fig. 1B) was placed in a vacuum chamber for 30 min to reach firm affixation, and the obtained device allowed for long-term bubble-free cell culture.

2.2. System used for the electrotaxis study

The system configuration has been adapted from previous studies [26] and illustrated in Fig. 2A. To monitor the temperature of the channels, a type-K thermocouple was clamped between the indium–tin–oxide (ITO) heater and the electrotaxis chip, which was placed on the ITO heater, which is transparent and does not interfere with microscopic observation of the cells. A proportional–integral–derivative controller (PID controller, Model TTM-J4-R-AB; Toho Electronics, Nagoya, Japan) controlled and maintained the ITO surface temperature at 37 °C. Subsequently, the chip together with the ITO heater was locked onto a programmable X–Y motorized stage, and the cell morphology and migration within the channels of the electrotaxis chip were monitored by an inverted phase-contrast microscope (Model CKX41; Olympus, Center Valley, PA) connected with a digital camera (Model 60D; Canon, Japan). For the application of the EF to the electrotaxis chip, Ag (anode side) and AgCl (cathode side) electrodes as electrical connections were inserted into the agar salt bridges, which were filled with 3% agar and connected to the cell culture medium. A home-built EF multiplexer was connected to a DC power supply (Model GPS-3030DQ; GW Instek, Taiwan) to provide independent and precise control of the current flow through individual channels. The multiplexer adjusted the current of each channel using a variable resistor that was serially connected to each channel. Then, the cells were subjected to dcEF stimulation according to the timeline in Fig. 2B.

2.3. Cell culture and maintenance

The human glioblastoma U-87 MG (U87) cell line was obtained from the Bioresource Collection and Research Center (BCRC, Taiwan). U87 cells were cultured in a complete medium of 90% minimum essential medium supplemented with 10% fetal bovine serum, 2 mM L-glutamine, 0.1 mM non-essential amino acids, and 1.0 mM sodium pyruvate (Thermo Fisher Scientific Inc., USA). The cells were incubated in flasks (Nunc, Roskilde, Denmark) at 37 °C in a humidified atmosphere of 5% CO_2 and were subcultured every 3–4 days. All experiments were performed using U87 cells within 10–25 passages from the source.

2.4. Cell viability assay

For cell viability measurement, U87 cells (2×10^4 cells/well) were seeded in 96-well black plates (Corning 3603, Costar) and incubated for 24 h at 37 °C in a humidified atmosphere with 5% CO_2. The culture medium in the 96-well plate was then replaced by doxycycline-containing medium, prepared as described below. Doxycycline

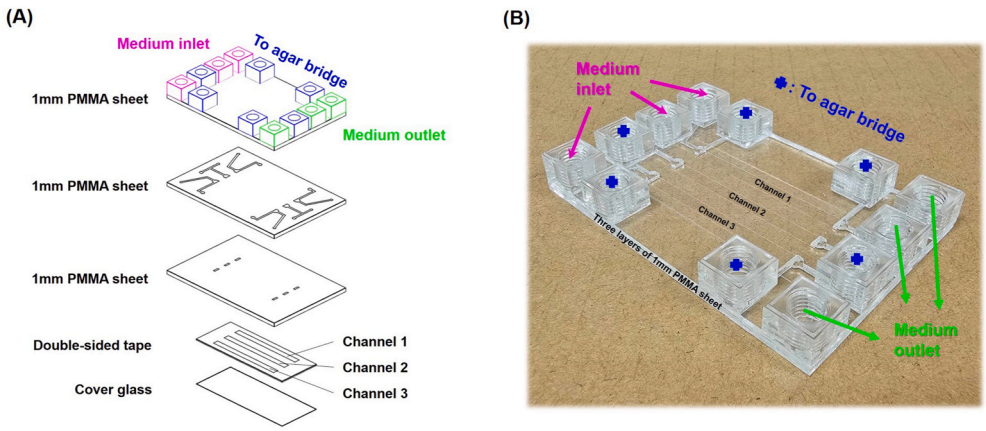

Fig. 1. Configuration of the electrotaxis chip. (A) Design for the assembly of the electrotaxis chip. The chip had connecting holes for the medium inlet, outlet, and agar salt bridges. The cells were cultured in the cell culture regions. The cell culture region's width, length, and thickness were 3 mm, 42 mm, and 70 μm, respectively. (B) Photograph of the electrotaxis chip.

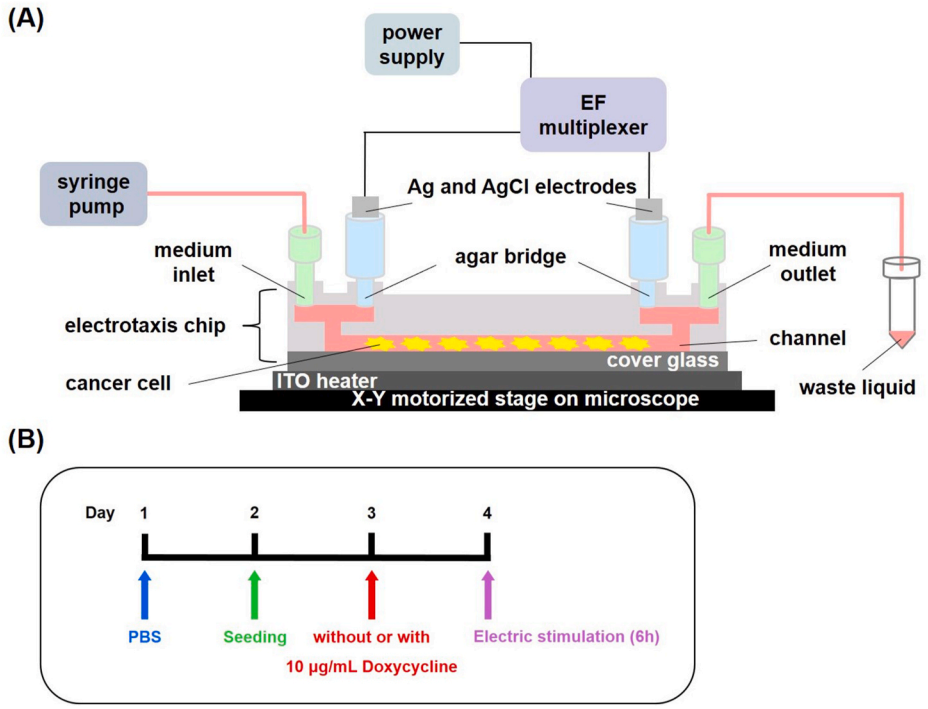

Fig. 2. The System used in the electrotaxis study. (A) The entire system's configuration. (B) The Experimental timeline of the electrical stimulation.

(D9891, Sigma-Aldrich) stock dissolved in DMSO was prepared and then diluted with the culture medium to final concentrations from 5 μg/mL to 200 μg/mL. The final DMSO concentration was below 0.4% for all the tests. The cells were then cultured for another 24 h. Then, the supernatant was removed and 100 μL of Live-Dead cell staining reagent (ALX-850-249, Enzo) was added to each well and incubated for 15 min at 37 °C. Subsequently, the fluorescence was measured using a fluorescence microplate reader (Synergy™ 2, BioTek).

2.5. Electrotaxis experiment

The detailed operation procedure used here was adopted from our previous study [52]. First, the U87 cells were resuspended in a complete medium and infused manually into the electrotaxis chip via the medium outlet. After 4 h of incubation, the cells adhered to the cover glass. Subsequently, a syringe pump was connected to the chip to pump fresh medium at a flow rate of 20 μL/h for 18 h to allow cell growth. To introduce the doxycycline inhibition, doxycycline with a final concentration of 10 μg/mL in culture medium was continuously infused through the channels at a flow rate of 20 μL/h for 24 h using a syringe pump. To prevent the effect of fluid flow on cell migration, the medium remained static during the electrotaxis experiment. In the channels of the electrotaxis chip, a voltage of 20 V was applied across the anode and the cathode to obtain an EF strength of 300 mV/mm. The acidity (pH) of the medium surrounding the electrodes remained unchanged during the EF stimulation [1]. The experimental setup was the same for the EF stimulated group (EF group) and the control (CTL) group, except the EF strength was set as 0 mV/mm in the latter. The strength of the EF applied in the cells was calculated based on the culture medium conductivity, as detailed in our previous report [17].

2.6. Quantitative analysis of MMP-2 and MMP-9 in U87 cells

The levels of MMP-2 and MMP-9 in the culture medium were measured using Human MMP2 (ab267813, Abcam) and Human MMP9 (ab246539, Abcam) ELISA kit. After the EF stimulation, air was pumped into the channel via the medium inlet, and the cell culture medium extruded from the outlet was collected and centrifuged at 2000×*g* for 10 min to remove floating cells. The obtained culture supernatants were stored at −20 °C until the analysis, as described below. First, the standard or sample was mixed with the MMP antibody and incubated at room temperature for 1 h. After washing, the TMB (3, 3′, 5, 5′-tetramethylbenzidine) development solution provided by the ELISA kits was added. After 10 min, the stop solution was added and the absorbance was measured at 450 nm using a microplate reader (SPECTROstar^{Nano}, BMG LABTECH). Before measuring the MMP levels of the samples, a calibration curve was obtained by measuring standard MMP solutions with concentrations from 0 to 80,000 pg/mL. The curve was then used to calculate the MMP concentrations of the samples. Three samples were obtained from three independent electrotaxis experiments. The measurement of each sample has three technical replicates and was repeated at least twice to ensure reproducibility and allow statistical evaluation.

2.7. Image analysis and data processing

2.7.1. Cell viability parameters analysis

The cell viability assayed by the Live-Dead staining was determined as follows. Live cells can be stained with a cell-permeable green fluorescent dye (excitation = 488 nm, emission = 518 nm). Dead cells can be easily stained by propidium iodide (PI), a cell non-permeable red fluorescent dye (excitation = 488 nm, emission = 615 nm). The following cell viability parameters were analyzed.

(1) F_{sample}: labeled with a green fluorescent dye and PI—the fluorescence at 518 nm in the experimental group.
(2) F_{min}: the fluorescence at 518 nm in the control group, in which all cells were alive and labeled with PI.
(3) F_{max}: the fluorescence at 518 nm in the control group, in which all cells were alive and labeled with the green fluorescent dye.

For cell viability analysis, the percentage of live cells was calculated from the fluorescence readings defined above as follows:

$$\%\ \text{Live cells} = \frac{F_{sample} - F_{min}}{F_{max} - F_{min}} \times 100\ \%$$

The data are expressed as the mean ± SD. In the electrotaxis assay, statistical inferences between cell groups with different treatments were conducted using the Student's t-test or one-way analysis of variance (ANOVA). In trajectory speed assay, two-way ANOVA using repeated measures was performed with EF stimulation and doxycycline treatment as independent variables. Significance was set at $P < 0.05$. Therefore, the asterisk (*) denotes $P < 0.05$, double asterisks (**) denote $P < 0.01$, and triple asterisks (***) denote $P < 0.001$.

2.7.2. Analysis of cell migration parameter

The time-lapse images (time interval, 10 min) obtained from phase-contrast microscopy were analyzed using Wimasis WimTaxis (Wimasis GmbH Munich, Germany), which is a tool that is used for the quantitative evaluation of cell migration and is suitable for analyzing time-lapse videos from phase-contrast observations. Over 100 cells from three independent experiments were analyzed in each experimental condition. The data were expressed as the mean ± SEM. The following cell migration parameters were analyzed.

(1) Distance of cell migration: the straight line distance (in μm) of the cell's centroid from the starting point to the final position in the entire test.
(2) Migration speed: the average cell migration distance per hour.
(3) Directedness: the average cosine θ (=Σcosθ/n). The vector of each cell from the starting point to the final position was first measured. The angle between the vector and that of the applied EF (positive to negative) is defined as θ, and the cell of numbers used for the analysis is n. The directedness of a cell moving toward the cathode and anode is +1 and −1, respectively.
(4) Trajectory length: the migration length of each cell was measured by the position differences between two consecutive time-lapse images, and then the migration lengths were added up to obtain the trajectory length.
(5) Trajectory speed: the total trajectory length divided by the total elapsed time, where the total trajectory length is the accumulated trajectory length of the entire track.

3. Results and discussion

3.1. Electrotaxis of human glioblastoma U87 cells

After the dcEF stimulation, the directedness of the U87 cells was 0.0 ± 0.1 and 0.3 ± 0.1 in the CTL and EF groups, respectively. The migration speed of U87 cells without the stimulation was 5.0 ± 0.7 μm/h and increased to 6.9 ± 0.6 μm/h under the stimulation (Fig. 3A). Our data (Fig. 3B) revealed that the U87 cells migrated toward the cathode under 300 mV/mm dcEF. Overall, there were significant differences between the directedness of the CTL and the EF groups (**$P < 0.01$). The migration speed of U87 cells under the EF stimulation was slightly higher than that detected in the CTL group (*$P < 0.05$).

Previous reports have shown that several types of cancer cells migrate under 50–400 mV/mm dcEFs [1,11,12,17,53]. For example, after dcEF stimulation, rat prostate cancer MAT-LyLu cells migrated toward the cathode [53], human breast cancer MDA-MB-231 cells and rat mammary adenocarcinoma MTLn3 cells migrated toward the anode [11], lung adenocarcinoma CL1-5 cells migrated toward the anode [1], human lung adenocarcinoma A549 cells migrated toward the cathode [12], oral squamous cell carcinoma HSC-3 cells migrated toward the cathode [17], and human U87 glioblastoma cells migrated toward the

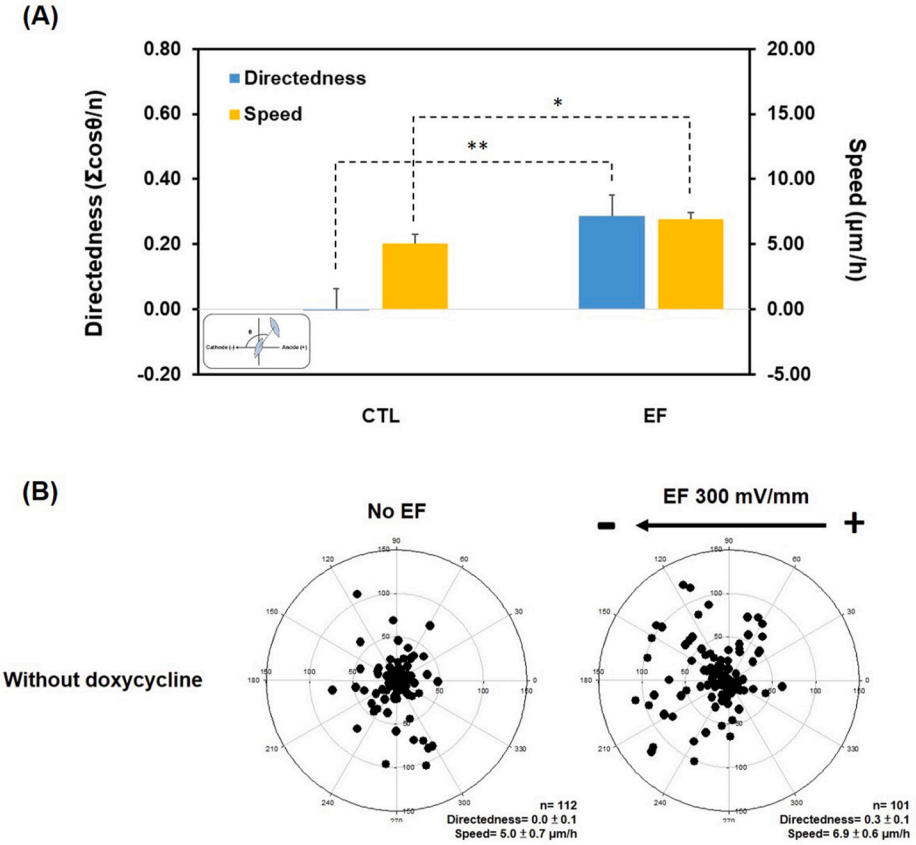

Fig. 3. Effect of EF on U87 cell migration. (A) The directedness and migration speed of U87 cells without (CTL) and with (EF) dcEF stimulation. Significance was set at $P < 0.05$. The asterisk (*) denotes $P < 0.05$, double asterisks (**) denote $P < 0.01$, and triple asterisks (***) denote $P < 0.001$. (B) Polar plots of the migration of U87 cells treated without doxycycline in the control (No EF) and EF groups. Each dot in the plots indicates the relative position of one cell in the experiments.

cathode [54]. In our study, U87 cells migrated toward the cathode and exhibited considerable electrotaxis after the dcEF stimulation. These results are in accordance with previous observations that various cancer cell types exhibit enhanced directional migration upon application of an external EF. The migration direction and speed depend on cell types and the origin of the dependency is poorly understood. However, there is a tendency that more malignant cancer cells respond more actively toward EF stimulation.

3.2. Viability of U87 cells after treatment with doxycycline

According to our previous study, human fetal lung fibroblast cell line MRC-5, human large cell lung carcinoma cell line NCI–H460, and human lung squamous cell carcinoma NCI–H520 cells incubated with 10 μg/mL doxycycline do not exhibit significant viability reduction [26]. In the present study, the effect of doxycycline on the viability of U87 cells was examined by treating cells with increasing concentrations of the drug (5–200 μg/mL) for 24 h. As shown in Fig. 4A, the viability of U87 cells decreased in response to high concentrations (80–200 μg/mL) of doxycycline. Before studying the effect of doxycycline on electrotaxis, we confirmed that doxycycline at 10 μg/mL had no noticeable effect on the U87 cell viability after 24 h of incubation (Fig. 4B). In accordance with the viability analysis, the cells' morphology did not exhibit apparent changes. A previous study has shown that doxycycline at low concentrations (5–15 μg/mL) has no noticeable effect on U87 cell viability [55]. Therefore, based on the observations described above, we selected non-cytotoxic concentrations of doxycycline (10 μg/mL) as the treatment concentration for the electrotaxis study and as the recommended optimum dose for future use. This concentration is significantly lower than the dose that caused an observable decrease in cell viability.

3.3. Effect of doxycycline on the electrotaxis of U87 cells

Cell migration and invasion are the initial steps of cancer metastasis [32]. Previous studies have demonstrated doxycycline's anti-migration and anti-metastasis effects [44,48,49,56]. Doxycycline inhibited cell migration in human breast cancer MDA-MB-435 cells [44], suppressed cell metastasis in prostate cancer [48], and inhibited cell metastasis in NCI–H446 lung cancer [49] and breast cancer [56] cells. In this study, U87 cells were grown in the electrotaxis chip and treated with or without doxycycline. The directedness of doxycycline-treated U87 cells without (Dox-CTL) and with (Dox-EF) dcEF stimulation is depicted in Fig. 5A. The directedness of the Dox-EF group was 0.1 ± 0.1 after dcEF stimulation. Compared with the EF group (Fig. 3), the Dox-EF group exhibited significantly reduced directedness (Fig. 5A) and less migration toward the cathode (Fig. 5B). Our results indicate that doxycycline hinders the EF-induced migration of U87 cells.

We further examined whether the reduced electrotactic response of U87 cells in the Dox-EF group was caused by reduced cell motility. A quantitative analysis of the trajectory speed of cells is shown in Fig. 6A. The trajectory speed of the CTL, EF, Dox-CTL, and Dox-EF groups was 21.9 ± 3.5, 25.4 ± 4.0, 36.8 ± 3.5, and 41.9 ± 4.2 μm/h, respectively. The U87 cells in the EF and the Dox-EF groups exhibited increased motility (1.6 fold) (Fig. 6A and B). This result suggests that the doxycycline treatment does not reduce cell motility. Our findings confirmed that doxycycline impeded the electrotactic migration of U87 cells while increasing the mobility of the cells. The above data suggest that doxycycline may regulate tumor progression by inhibiting cell electrotaxis but not activity. Therefore, we further examined EF stimulation's effect on proteins highly expressed in malignant glioblastoma cells.

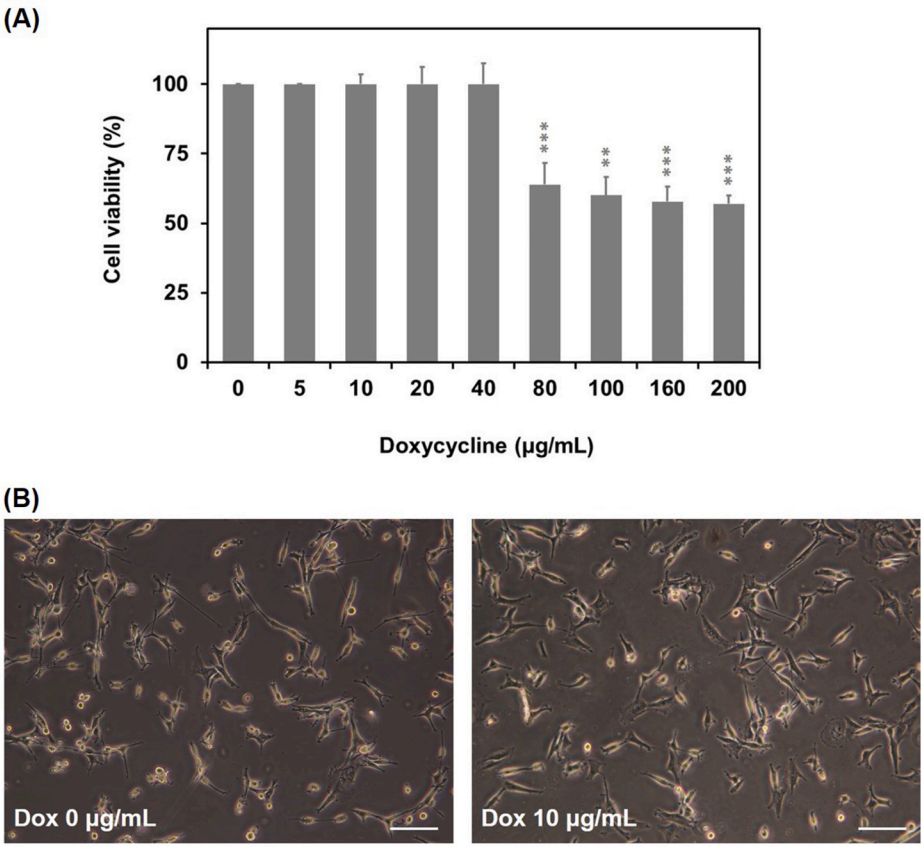

Fig. 4. Effect of doxycycline on U87 cell viability. (A) Viability of U87 cells after treatment with doxycycline at different concentrations. Significance was set at $P < 0.05$. The asterisk (*) denotes $P < 0.05$, double asterisks (**) denote $P < 0.01$, and triple asterisks (***) denote $P < 0.001$. (B) The morphology of U87 cells treated with doxycycline (Dox) at 0 and 10 μg/mL for 24 h shows no apparent difference. Scale bar: 200 μm.

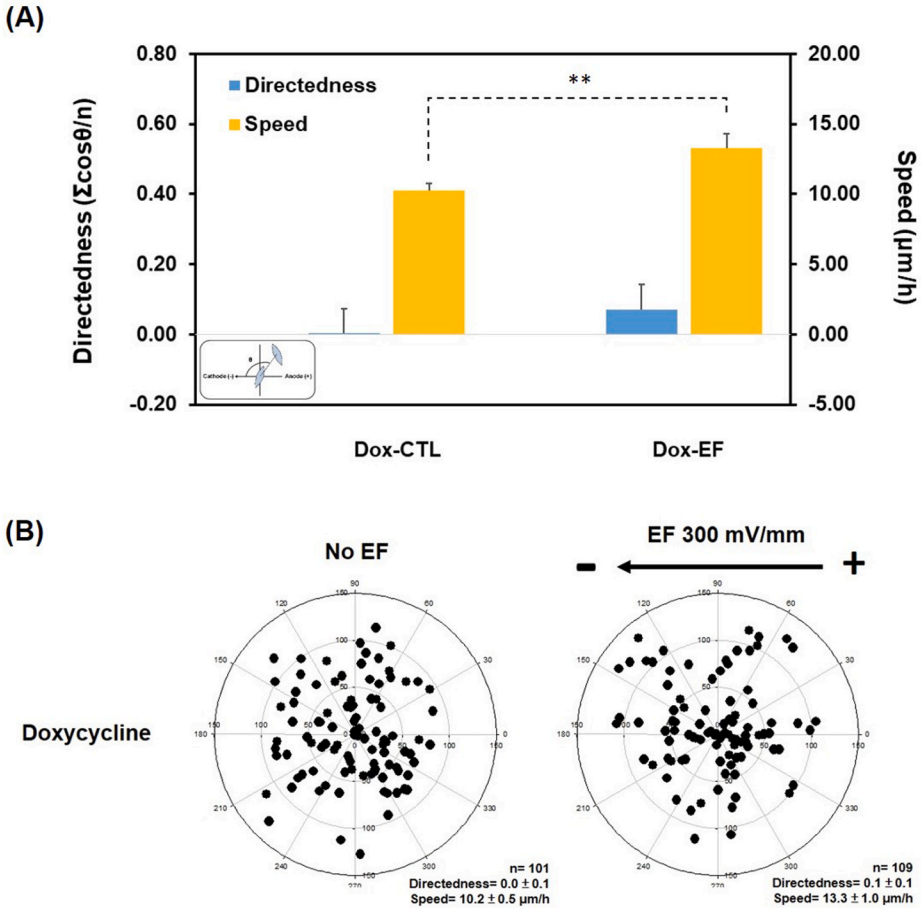

Fig. 5. Effect of doxycycline on U87 cell migration. (A) The directedness and migration speed of U87 cells treated with doxycycline without (Dox-CTL) and with (Dox-EF) dcEF stimulation. Significance was set at $P < 0.05$. The asterisk (*) denotes $P < 0.05$, double asterisks (**) denote $P < 0.01$, and triple asterisks (***) denote $P < 0.001$. (B) Polar plots of the migration of U87 cells in the Dox-CTL and Dox-EF groups. Each dot in the plots indicates the relative position of one cell in the experiments.

3.4. Expression of MMP-2 and MMP-9 in U87 cells

In this study, we selected non-cytotoxic concentrations of doxycycline to evaluate its effect on the electrotaxis of U87 cells. Previous studies have shown that doxycycline inhibits various MMPs [57–59]. MMPs play critical roles in tumor growth [60], migration [61], invasion [62], and angiogenesis [63]. Thus, the downregulation of MMP expression and activity may inhibit the migration of cancer cells [64–66]. Specifically, MMP-2 and MMP-9 enhance glioma tumor proliferation, migration, invasion, and angiogenesis [67]. Based on the findings of these previous works, we further investigated the effects of physical stimulation (i.e., EF), chemical stimulation (i.e., doxycycline), and combined stimulation on the expression levels of MMP-2 and MMP-9.

Fig. 6C depicts the MMP-2 and MMP-9 levels in the CTL, EF, Dox-CTL, and Dox-EF groups. We found that the levels of MMP-2 were similar among all groups. In contrast, after the electrical stimulation, the U87 cells expressed significantly higher levels of MMP-9 compared with the CTL group (***$P < 0.001$). The EF-enhanced MMP-9 expression is consistent with the observation that malignant cancer cells migrate actively in physiological EFs [8,17,26]. Our result also showed that the EF-enhanced high level of MMP-9 was greatly reduced in the Dox-EF group compared with the EF group (***$P < 0.001$). This result indicated that EF alone considerably upregulated MMP-9 and that the doxycycline treatment mostly counteracted the enhancement. Moreover, although the motility of the U87 cells was enhanced by doxycycline, the MMP-9 level was not increased in the Dox-CTL group compared with the CTL group. Previous reports have indicated that the suppression of the MMP-9 activity inhibited the wound healing migration (*in vitro* scratch assay) of human lung cancer cells [68], human MCF-7 breast cancer cells [69], and human hepatocellular carcinoma cells [70], and suppressed the migration of MDA-MB-231 human breast cancer cells in an *in vitro* transwell migration assay [71]. These results agree with ours, as the downregulation of MMP-9 reduced the migration potential of U87 cells. Oh et al. reported that, after 12-O-tetradecanoylphorbol-13-acetate (TPA) treatment, MMP-9 was significantly upregulated in TPC-1 human thyroid cancer cells and MCF-7 human breast cancer cells, whereas the expression of MMP-2 remained unaltered. Furthermore, silibinin inhibited TPA-induced cell migration and MMP-9 expression in TPC-1 and MCF-7 cells [72]. The finding of Oh et al. was similar to ours in that the responses of MMP-2 and MMP-9 to external stimuli differed. Our results suggest that MMP-9 is correlated with the doxycycline-induced reduction of U87 cells electrotaxis. However, reduction of EF-enhanced MMP-9 may not be the cause of the electrotaxis reduction. This is because MMP-9 is a peptidase and, in this work, the electrotaxis of the U87 cells on the glass surface involved no extracellular matrix proteins. The proteins that participates in cell adhesion and cellular motility, such as focal adhesion kinase (FAK), may be involved.

Previous reports have indicated that doxycycline inhibits human cancer cell migration by inhibiting the FAK signaling pathways [73,74]. FAK is a crucial protein tyrosine kinase that regulates the migration of cancer cells [75]. Moreover, FAK and its phosphorylation play vital roles in the secretion of MMP, which is associated with activated cancer cell

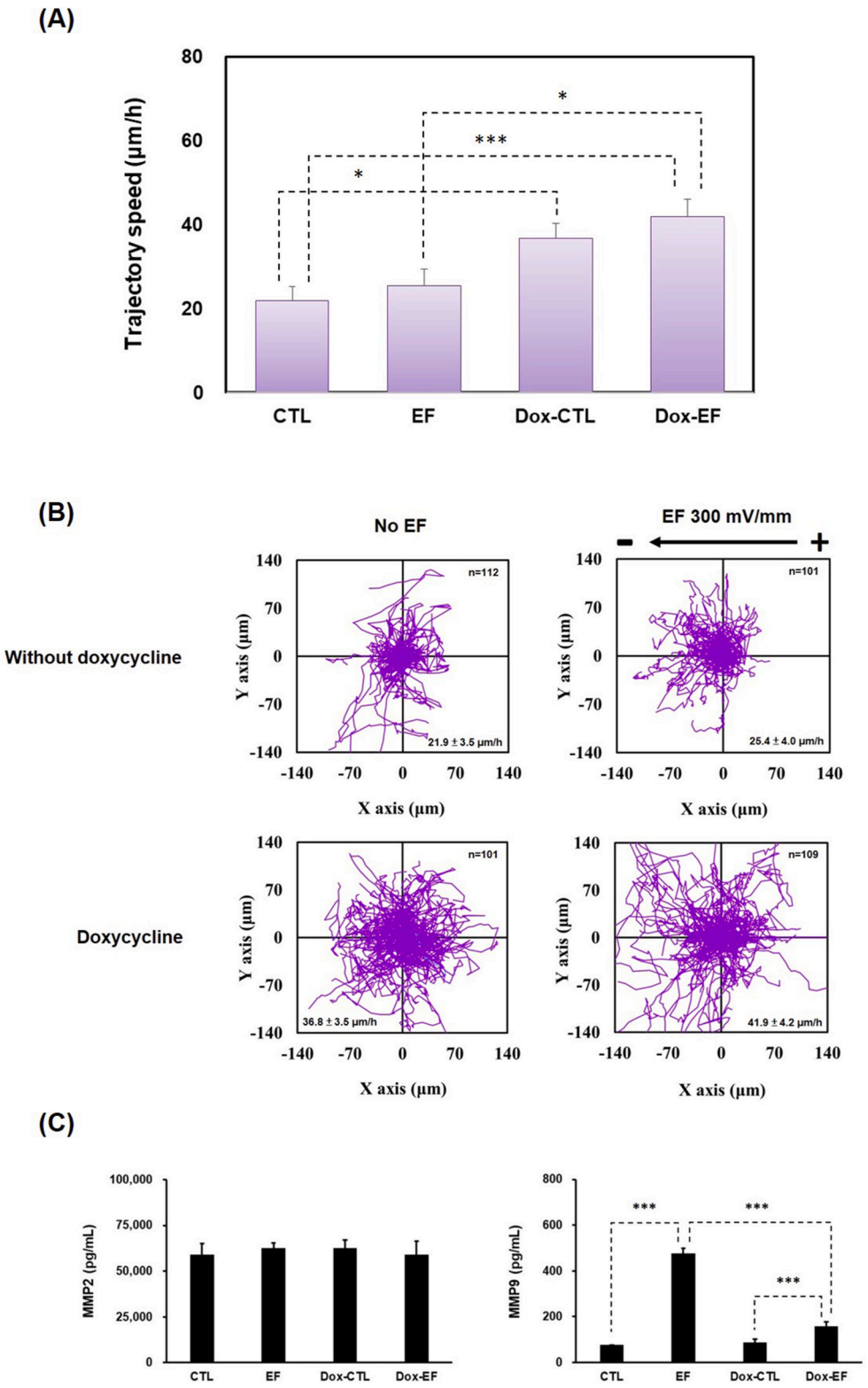

Fig. 6. The effect of U87 cells treated without and with doxycycline (Dox) in the control (CTL) and electric field (EF) groups. (A) The trajectory speed of U87 cells in the CTL, EF, Dox-CTL, and Dox-EF groups. (B) Effect of doxycycline and EF stimulation on the migration trajectories of the U87 cells. (C) MMP-2 and MMP-9 levels in the CTL, EF, and doxycycline-treated groups. Significance was set at $P < 0.05$. The asterisk (*) denotes $P < 0.05$, double asterisks (**) denote $P < 0.01$, and triple asterisks (***) denote $P < 0.001$.

migration [76]. For example, Sun et al. indicated that doxycycline inhibits melanoma migration by inhibiting the expression and phosphorylation of FAK and the downregulation of MMP-2 and MMP-9 [73]. Furthermore, Wang et al. reported that doxycycline also partly inhibits the migration of human leukemic cells by suppressing the expression and phosphorylation of FAK and inhibiting MMP-2 and MMP-9 [74]. FAK is generally considered to be up-stream of MMP-9. Based on our findings and those from the previous studies, the combined effect of EF

and doxycycline on the FAK protein expression level and the phosphorylation requires further investigation.

4. Conclusion

This study revealed that U87 cells migrated toward the cathode under an EF strength of 300 mV/mm. Moreover, doxycycline treatment reduced electrotaxis and reduced EF-enhanced MMP-9 levels of U87 cells. Although the molecular mechanisms underlying the inhibition of glioblastoma cell electrotaxis by doxycycline are still unclear, our study pointed out that understanding the role of doxycycline and MMP in EF-induced U87 cell migration could help enhance the anti-metastasis treatment of cancers in the future. Especially, our result correlated the reduced EF responses of glioblastoma cells with antibiotic treatment and pointed out that MMP-9 is a potential leverage point for reducing cancer metastasis *in vivo*.

CRediT authorship contribution statement

Hui-Fang Chang: Formal analysis, Investigation, Methodology, Validation, Visualization, Writing – original draft. **Ji-Yen Cheng:** Conceptualization, Data curation, Funding acquisition, Project administration, Resources, Writing – review & editing.

Declaration of competing interest

The authors declare no conflicts of interest.

Data availability

Data will be made available on request.

Acknowledgments

The authors thank the partial financial support from the National Science and Technology Council, Taiwan (Contract numbers: MOST 110-2113-M-001-021 and MOST 111-2113-M-001-046).

References

[1] C.W. Huang, J.Y. Cheng, M.H. Yen, T.H. Young, Electrotaxis of lung cancer cells in a multiple-electric-field chip, Biosens. Bioelectron. 24 (2009) 3510–3516, https://doi.org/10.1016/j.bios.2009.05.001.
[2] B. Cortese, I.E. Palama, S. D'Amone, G. Gigli, Influence of electrotaxis on cell behaviour, Integr. Biol. 6 (2014) 817–830, https://doi.org/10.1039/c4ib00142g.
[3] M. Zhao, J.V. Forrester, C.D. McCaig, A small, physiological electric field orients cell division, Proc. Natl. Acad. Sci. U. S. A. 96 (1999) 4942–4946, https://doi.org/10.1073/pnas.96.9.4942.
[4] H.F. Chang, Y.S. Lee, T.K. Tang, J.Y. Cheng, Pulsed DC electric field-induced differentiation of cortical neural precursor cells, PLoS One 11 (2016) e0158133, https://doi.org/10.1371/journal.pone.0158133.
[5] L. Yao, L. Shanley, C. McCaig, M. Zhao, Small applied electric fields guide migration of hippocampal neurons, J. Cell. Physiol. 216 (2008) 527–535, https://doi.org/10.1002/jcp.21431.
[6] C. Yang, L. Wang, W. Weng, S. Wang, Y. Ma, Q. Mao, G. Gao, R. Chen, J. Feng, Steered migration and changed morphology of human astrocytes by an applied electric field, Exp. Cell Res. 374 (2019) 282–289, https://doi.org/10.1016/j.yexcr.2018.11.029.
[7] K.R. Ammann, M.J. Slepian, Vascular endothelial and smooth muscle cell galvanotactic response and differential migratory behavior, Exp. Cell Res. 399 (2021) 112447, https://doi.org/10.1016/j.yexcr.2020.112447.
[8] H. Clancy, M. Pruski, B. Lang, J. Ching, C.D. McCaig, Glioblastoma cell migration is directed by electrical signals, Exp. Cell Res. 406 (2021) 112736, https://doi.org/10.1016/j.yexcr.2021.112736.
[9] F. Hilpert, A. Heiser, W. Wieckhorst, N. Arnold, D. Kabelitz, W. Jonat, J. Pfisterer, The impact of electrical charge on the viability and physiology of dendritic cells, Scand. J. Immunol. 62 (2005) 399–406, https://doi.org/10.1111/j.1365-3083.2005.01677.x.
[10] E.I. Finkelstein, P.H. Chao, C.T. Hung, J.C. Bulinski, Electric field-induced polarization of charged cell surface proteins does not determine the direction of galvanotaxis, Cell Motil Cytoskeleton 64 (2007) 833–846, https://doi.org/10.1002/cm.20227.
[11] J. Pu, C.D. McCaig, L. Cao, Z. Zhao, J.E. Segall, M. Zhao, EGF receptor signalling is essential for electric-field-directed migration of breast cancer cells, J. Cell Sci. 120 (2007) 3395–3403, https://doi.org/10.1242/jcs.002774.
[12] X. Yan, J. Han, Z. Zhang, J. Wang, Q. Cheng, K. Gao, Y. Ni, Y. Wang, Lung cancer A549 cells migrate directionally in DC electric fields with polarized and activated EGFRs, Bioelectromagnetics 30 (2009) 29–35, https://doi.org/10.1002/bem.20436.
[13] N. Ozkucur, S. Perike, P. Sharma, R.H. Funk, Persistent directional cell migration requires ion transport proteins as direction sensors and membrane potential differences in order to maintain directedness, BMC Cell Biol. 12 (2011) 4, https://doi.org/10.1186/1471-2121-12-4.
[14] F. Li, H. Wang, L. Li, C. Huang, J. Lin, G. Zhu, Z. Chen, N. Wu, H. Feng, Superoxide plays critical roles in electrotaxis of fibrosarcoma cells via activation of ERK and reorganization of the cytoskeleton, Free Radic. Biol. Med. 52 (2012) 1888–1896, https://doi.org/10.1016/j.freeradbiomed.2012.02.047.
[15] Y.S. Sun, S.W. Peng, K.H. Lin, J.Y. Cheng, Electrotaxis of lung cancer cells in ordered three-dimensional scaffolds, Biomicrofluidics 6 (2012) 14102–1410214, https://doi.org/10.1063/1.3671399.
[16] C. Martin-Granados, A.R. Prescott, N. Van Dessel, A. Van Eynde, M. Arocena, I. P. Klaska, J. Gornemann, M. Beullens, M. Bollen, J.V. Forrester, C.D. McCaig, A role for PP1/NIPP1 in steering migration of human cancer cells, PLoS One 7 (2012) e40769, https://doi.org/10.1371/journal.pone.0040769.
[17] H.F. Tsai, S.W. Peng, C.Y. Wu, H.F. Chang, J.Y. Cheng, Electrotaxis of oral squamous cell carcinoma cells in a multiple-electric-field chip with uniform flow field, Biomicrofluidics 6 (2012) 34116, https://doi.org/10.1063/1.4749826.
[18] D. Wu, X. Ma, F. Lin, DC electric fields direct breast cancer cell migration, induce EGFR polarization, and increase the intracellular level of calcium ions, Cell Biochem. Biophys. 67 (2013) 1115–1125, https://doi.org/10.1007/s12013-013-9615-7.
[19] Y.C. Kao, M.H. Hsieh, C.C. Liu, H.J. Pan, W.Y. Liao, J.Y. Cheng, P.L. Kuo, C.H. Lee, Modulating chemotaxis of lung cancer cells by using electric fields in a microfluidic device, Biomicrofluidics 8 (2014) 024107, https://doi.org/10.1063/1.4870401.
[20] M.S. Kim, M.H. Lee, B.J. Kwon, H.J. Seo, M.A. Koo, K.E. You, D. Kim, J.C. Park, Effects of direct current electric-field using ITO plate on breast cancer cell migration, Biomater. Res. 18 (2014) 10, https://doi.org/10.1186/2055-7124-18-10.
[21] Y. Li, T. Xu, H. Zou, X. Chen, D. Sun, M. Yang, Cell migration microfluidics for electrotaxis-based heterogeneity study of lung cancer cells, Biosens. Bioelectron. 89 (2017) 837–845, https://doi.org/10.1016/j.bios.2016.10.002.
[22] Y. Li, T. Xu, X. Chen, S. Lin, M. Cho, D. Sun, M. Yang, Effects of direct current electric fields on lung cancer cell electrotaxis in a PMMA-based microfluidic device, Anal. Bioanal. Chem. 409 (2017) 2163–2178, https://doi.org/10.1007/s00216-016-0162-0.
[23] L. Li, K. Zhang, C. Lu, Q. Sun, S. Zhao, L. Jiao, R. Han, C. Lin, J. Jiang, M. Zhao, Y. He, Caveolin-1-mediated STAT3 activation determines electrotaxis of human lung cancer cells, Oncotarget 8 (2017) 95741–95754, https://doi.org/10.18632/oncotarget.21306.
[24] Y. Li, W.K. Yu, L. Chen, Y.S. Chan, D. Liu, C.C. Fong, T. Xu, G. Zhu, D. Sun, M. Yang, Electrotaxis of tumor-initiating cells of H1975 lung adenocarcinoma cells is associated with both activation of stretch-activated cation channels (SACCs) and internal calcium release, Bioelectrochemistry 124 (2018) 80–92, https://doi.org/10.1016/j.bioelechem.2018.03.013.
[25] J.G. Lyon, S.L. Carroll, N. Mokarram, R.V. Bellamkonda, Electrotaxis of glioblastoma and medulloblastoma spheroidal aggregates, Sci. Rep. 9 (2019) 5309, https://doi.org/10.1038/s41598-019-41505-6.
[26] H.F. Chang, H.T. Cheng, H.Y. Chen, W.K. Yeung, J.Y. Cheng, Doxycycline inhibits electric field-induced migration of non-small cell lung cancer (NSCLC) cells, Sci. Rep. 9 (2019) 8094, https://doi.org/10.1038/s41598-019-44505-8.
[27] H.F. Tsai, I.J. C, A.Q. Shen, Voltage-gated ion channels mediate the electrotaxis of glioblastoma cells in a hybrid PMMA/PDMS microdevice, APL Bioeng. 4 (2020) 036102, https://doi.org/10.1063/5.0004893.
[28] M. Szatkowski, M. Mycielska, R. Knowles, A.L. Kho, M.B. Djamgoz, Electrophysiological recordings from the rat prostate gland in vitro: identified single-cell and transepithelial (lumen) potentials, BJU Int. 86 (2000) 1068–1075, https://doi.org/10.1046/j.1464-410x.2000.00889.x.
[29] Q. Wang, J.D. Horisberger, M. Maillard, H.R. Brunner, B.C. Rossier, M. Burnier, Salt- and angiotensin II-dependent variations in amiloride-sensitive rectal potential difference in mice, Clin. Exp. Pharmacol. Physiol. 27 (2000) 60–66, https://doi.org/10.1046/j.1440-1681.2000.03204.x.
[30] F.J. Al-Bazzaz, C. Gailey, Ion transport by sheep distal airways in a miniature chamber, Am. J. Physiol. Lung Cell Mol. Physiol. 281 (2001) L1028–L1034, https://doi.org/10.1152/ajplung.2001.281.4.L1028.
[31] H. Dillekas, M.S. Rogers, O. Straume, Are 90% of deaths from cancer caused by metastases? Cancer Med. 8 (2019) 5574–5576, https://doi.org/10.1002/cam4.2474.
[32] F. van Zijl, G. Krupitza, W. Mikulits, Initial steps of metastasis: cell invasion and endothelial transmigration, Mutat. Res. 728 (2011) 23–34, https://doi.org/10.1016/j.mrrev.2011.05.002.
[33] W. Diao, X. Tong, C. Yang, F. Zhang, C. Bao, H. Chen, L. Liu, M. Li, F. Ye, Q. Fan, J. Wang, Z.C. Ou-Yang, Behaviors of glioblastoma cells in in vitro microenvironments, Sci. Rep. 9 (2019) 85, https://doi.org/10.1038/s41598-018-36347-7.
[34] L. Carr, S.M. Bardet, R.C. Burke, D. Arnaud-Cormos, P. Leveque, R.P. O'Connor, Calcium-independent disruption of microtubule dynamics by nanosecond pulsed electric fields in U87 human glioblastoma cells, Sci. Rep. 7 (2017) 41267, https://doi.org/10.1038/srep41267.

[35] M. Soueid, M.C.F. Dobbelaar, S. Bentouati, S.M. Bardet, R.P. O'Connor, D. Bessieres, J. Paillol, P. Leveque, D. Arnaud-Cormos, Delivery devices for exposure of biological cells to nanosecond pulsed electric fields, Med. Biol. Eng. Comput. 56 (2018) 85–97, https://doi.org/10.1007/s11517-017-1676-0.
[36] A.A. Petrov, A.A. Moraleva, N.V. Antipova, R.K. Amirov, I.S. Samoylov, S. Y. Savinov, The action of the pulsed electric field of the subnanosecond range on human tumor cells, Bioelectromagnetics 43 (2022) 327–335, https://doi.org/10.1002/bem.22408.
[37] J.S. Rao, Molecular mechanisms of glioma invasiveness: the role of proteases, Nat. Rev. Cancer 3 (2003) 489–501, https://doi.org/10.1038/nrc1121.
[38] H. Song, Y. Li, J. Lee, A.L. Schwartz, G. Bu, Low-density lipoprotein receptor-related protein 1 promotes cancer cell migration and invasion by inducing the expression of matrix metalloproteinases 2 and 9, Cancer Res. 69 (2009) 879–886, https://doi.org/10.1158/0008-5472.CAN-08-3379.
[39] E. Tabouret, F. Boudouresque, M. Barrie, M. Matta, C. Boucard, A. Loundou, A. Carpentier, M. Sanson, P. Metellus, D. Figarella-Branger, L. Ouafik, O. Chinot, Association of matrix metalloproteinase 2 plasma level with response and survival in patients treated with bevacizumab for recurrent high-grade glioma, Neuro Oncol. 16 (2014) 392–399, https://doi.org/10.1093/neuonc/not226.
[40] X. Lei, L. Chang, W. Ye, C. Jiang, Z. Zhang, Raf kinase inhibitor protein (RKIP) inhibits the cell migration and invasion in human glioma cell lines in vitro, Int. J. Clin. Exp. Pathol. 8 (2015) 14214–14220.
[41] G. Musumeci, G. Magro, V. Cardile, M. Coco, R. Marzagalli, P. Castrogiovanni, R. Imbesi, A.C. Graziano, F. Barone, M. Di Rosa, S. Castorina, A. Castorina, Characterization of matrix metalloproteinase-2 and -9, ADAM-10 and N-cadherin expression in human glioblastoma multiforme, Cell Tissue Res. 362 (2015) 45–60, https://doi.org/10.1007/s00441-015-2197-5.
[42] T. Hamad, B. Hellmark, A. Nilsdotter-Augustinsson, B. Soderquist, Antibiotic susceptibility among Staphylococcus epidermidis isolated from prosthetic joint infections, with focus on doxycycline, APMIS 123 (2015) 1055–1060, https://doi.org/10.1111/apm.12465.
[43] M. Pradier, S. Nguyen, O. Robineau, M. Titecat, N. Blondiaux, M. Valette, C. Loiez, E. Beltrand, H. Dezeque, H. Migaud, E. Senneville, Suppressive antibiotic therapy with oral doxycycline for Staphylococcus aureus prosthetic joint infection: a retrospective study of 39 patients, Int. J. Antimicrob. Agents 50 (2017) 447–452, https://doi.org/10.1016/j.ijantimicag.2017.04.019.
[44] R.S. Fife, G.W. Sledge Jr., Effects of doxycycline on in vitro growth, migration, and gelatinase activity of breast carcinoma cells, J. Lab. Clin. Med. 125 (1995) 407–411.
[45] R.S. Fife, B.T. Rougraff, C. Proctor, G.W. Sledge Jr., Inhibition of proliferation and induction of apoptosis by doxycycline in cultured human osteosarcoma cells, J. Lab. Clin. Med. 130 (1997) 530–534, https://doi.org/10.1016/s0022-2143(97)90130-x.
[46] R.S. Fife, G.W. Sledge Jr., Effects of doxycycline on cancer cells in vitro and in vivo, Adv. Dent. Res. 12 (1998) 94–96, https://doi.org/10.1177/08959374980120012801.
[47] W.C. Duivenvoorden, S.V. Popovic, S. Lhotak, E. Seidlitz, H.W. Hirte, R.G. Tozer, G. Singh, Doxycycline decreases tumor burden in a bone metastasis model of human breast cancer, Cancer Res. 62 (2002) 1588–1591.
[48] B.L. Lokeshwar, M.G. Selzer, B.Q. Zhu, N.L. Block, L.M. Golub, Inhibition of cell proliferation, invasion, tumor growth and metastasis by an oral non-antimicrobial tetracycline analog (COL-3) in a metastatic prostate cancer model, Int. J. Cancer 98 (2002) 297–309, https://doi.org/10.1002/ijc.10168.
[49] Y. Qin, Q. Zhang, S. Lee, W.L. Zhong, Y.R. Liu, H.J. Liu, D. Zhao, S. Chen, T. Xiao, J. Meng, X.S. Jing, J. Wang, B. Sun, T.T. Dai, C. Yang, T. Sun, H.G. Zhou, Doxycycline reverses epithelial-to-mesenchymal transition and suppresses the proliferation and metastasis of lung cancer cells, Oncotarget 6 (2015) 40667–40679, https://doi.org/10.18632/oncotarget.5842.
[50] C.W. Huang, H.Y. Chen, M.H. Yen, J.J. Chen, T.H. Young, J.Y. Cheng, Gene expression of human lung cancer cell line CL1-5 in response to a direct current electric field, PLoS One 6 (2011) e25928, https://doi.org/10.1371/journal.pone.0025928.
[51] H.F. Tsai, C.W. Huang, H.F. Chang, J.J. Chen, C.H. Lee, J.Y. Cheng, Evaluation of EGFR and RTK signaling in the electrotaxis of lung adenocarcinoma cells under direct-current electric field stimulation, PLoS One 8 (2013) e73418, https://doi.org/10.1371/journal.pone.0073418.
[52] H.F. Chang, S.E. Chou, J.Y. Cheng, Electric-field-induced neural precursor cell differentiation in microfluidic devices, J. Vis. Exp. (2021) e61917, https://doi.org/10.3791/61917.
[53] M.B.A. Djamgoz, M. Mycielska, Z. Madeja, S.P. Fraser, W. Korohoda, Directional movement of rat prostate cancer cells in direct-current electric field: involvement of voltagegated Na+ channel activity, J. Cell Sci. 114 (2001) 2697–2705, https://doi.org/10.1242/jcs.114.14.2697.
[54] F. Li, T. Chen, S. Hu, J. Lin, R. Hu, H. Feng, Superoxide mediates direct current electric field-induced directional migration of glioma cells through the activation of AKT and ERK, PLoS One 8 (2013) e61195, https://doi.org/10.1371/journal.pone.0061195.
[55] A. Wang-Gillam, E. Siegel, D.A. Mayes, L.F. Hutchins, Y.H. Zhou, Anti-tumor effect of doxycycline on glioblastoma cells, J. Cancer Mol. 3 (2007) 147–153.
[56] W. Zhong, S. Chen, Y. Qin, H. Zhang, H. Wang, J. Meng, L. Huai, Q. Zhang, T. Yin, Y. Lei, J. Han, L. He, B. Sun, H. Liu, Y. Liu, H. Zhou, T. Sun, C. Yang, Doxycycline inhibits breast cancer EMT and metastasis through PAR-1/NF-kappaB/miR-17/E-cadherin pathway, Oncotarget 8 (2017) 104855–104866, https://doi.org/10.18632/oncotarget.20418.
[57] R. Hanemaaijer, H. Visser, P. Koolwijk, T. Sorsa, T. Salo, L.M. Golub, V.W. van Hinsbergh, Inhibition of MMP synthesis by doxycycline and chemically modified tetracyclines (CMTs) in human endothelial cells, Adv. Dent. Res. 12 (1998) 114–118, https://doi.org/10.1177/08959374980120010301.
[58] J. Liu, W. Xiong, L. Baca-Regen, H. Nagase, B.T. Baxter, Mechanism of inhibition of matrix metalloproteinase-2 expression by doxycycline in human aortic smooth muscle cells, J. Vasc. Surg. 38 (2003) 1376–1383, https://doi.org/10.1016/s0741-5214(03)01022-x.
[59] H.S. Kim, L. Luo, S.C. Pflugfelder, D.Q. Li, Doxycycline inhibits TGF-beta1-induced MMP-9 via Smad and MAPK pathways in human corneal epithelial cells, Invest. Ophthalmol. Vis. Sci. 46 (2005) 840–848, https://doi.org/10.1167/iovs.04-0929.
[60] N.E. Sounni, L. Devy, A. Hajitou, F. Frankenne, C. Munaut, C. Gilles, C. Deroanne, E.W. Thompson, J.M. Foidart, A. Noel, MT1-MMP expression promotes tumor growth and angiogenesis through an up-regulation of vascular endothelial growth factor expression, Faseb. J. 16 (2002) 555–564, https://doi.org/10.1096/fj.01-0790com.
[61] K. Nabeshima, T. Inoue, Y. Shimao, T. Sameshima, Matrix metalloproteinases in tumor invasion: role for cell migration, Pathol. Int. 52 (2002) 255–264, https://doi.org/10.1046/j.1440-1827.2002.01343.x.
[62] M.R. Emmert-Buck, M.J. Roth, Z. Zhuang, E. Campo, J. Rozhin, B.F. Sloane, L. A. Liotta, W.G. Stetler-Stevenson, Increased gelatinase A (MMP-2) and cathepsin B activity in invasive tumor regions of human colon cancer samples, Am. J. Pathol. 145 (1994) 1285–1290.
[63] E.I. Deryugina, J.P. Quigley, Tumor angiogenesis: MMP-mediated induction of intravasation- and metastasis-sustaining neovasculature, Matrix Biol. 44–46 (2015) 94–112, https://doi.org/10.1016/j.matbio.2015.04.004.
[64] C.L. Liao, K.C. Lai, A.C. Huang, J.S. Yang, J.J. Lin, S.H. Wu, W. Gibson Wood, J. G. Lin, J.G. Chung, Gallic acid inhibits migration and invasion in human osteosarcoma U-2 OS cells through suppressing the matrix metalloproteinase-2/-9, protein kinase B (PKB) and PKC signaling pathways, Food Chem. Toxicol. 50 (2012) 1734–1740, https://doi.org/10.1016/j.fct.2012.02.033.
[65] M.M. Lee, Y.Y. Chen, P.Y. Liu, S. Hsu, M.J. Sheu, Pipoxolan inhibits CL1-5 lung cancer cells migration and invasion through inhibition of MMP-9 and MMP-2, Chem. Biol. Interact. 236 (2015) 19–30, https://doi.org/10.1016/j.cbi.2015.04.012.
[66] I.K. Sani, S.H. Marashi, F. Kalalinia, Solamargine inhibits migration and invasion of human hepatocellular carcinoma cells through down-regulation of matrix metalloproteinases 2 and 9 expression and activity, Toxicol. Vitro 29 (2015) 893–900, https://doi.org/10.1016/j.tiv.2015.03.012.
[67] J.H. Uhm, N.P. Dooley, J.G. Villemure, V.W. Yong, Mechanisms of glioma invasion: role of matrix-metalloproteinases, Can. J. Neurol. Sci. 24 (1997) 3–15, https://doi.org/10.1017/s0317167100021028.
[68] M. Zhao, Y. Gao, L. Wang, S. Liu, B. Han, L. Ma, Y. Ling, S. Mao, X. Wang, Overexpression of integrin-linked kinase promotes lung cancer cell migration and invasion via NF-kappaB-mediated upregulation of matrix metalloproteinase-9, Int. J. Med. Sci. 10 (2013) 995–1002, https://doi.org/10.7150/ijms.5963.
[69] S.Y. Jang, A. Kim, J.K. Kim, C. Kim, Y.H. Cho, J.H. Kim, C.H. Kim, J.Y. Lee, Metformin inhibits tumor cell migration via down-regulation of MMP9 in tamoxifen-resistant breast cancer cells, Anticancer Res. 34 (2014) 4127–4134.
[70] P.C. Ju, Y.C. Ho, P.N. Chen, H.L. Lee, S.Y. Lai, S.F. Yang, C.B. Yeh, Kaempferol inhibits the cell migration of human hepatocellular carcinoma cells by suppressing MMP-9 and Akt signaling, Environ. Toxicol. 36 (2021) 1981–1989, https://doi.org/10.1002/tox.23316.
[71] M. Izdebska, W. Zielinska, A. Krajewski, M. Halas-Wisniewska, K. Mikolajczyk, M. Gagat, A. Grzanka, Downregulation of MMP-9 enhances the anti-migratory effect of cyclophosphamide in MDA-MB-231 and MCF-7 breast cancer cell lines, Int. J. Mol. Sci. 22 (2021), https://doi.org/10.3390/ijms222312783.
[72] S.J. Oh, S.P. Jung, J. Han, S. Kim, J.S. Kim, S.J. Nam, J.E. Lee, J.H. Kim, Silibinin inhibits TPA-induced cell migration and MMP-9 expression in thyroid and breast cancer cells, Oncol. Rep. 29 (2013) 1343–1348, https://doi.org/10.3892/or.2013.2252.
[73] T. Sun, N. Zhao, C.S. Ni, X.L. Zhao, W.Z. Zhang, X. Su, D.F. Zhang, Q. Gu, B.C. Sun, Doxycycline inhibits melanoma cells' adhesion and migration by inhibiting focal adhesion kinase's expression and phosphorylation (FAK), Cancer Lett. 285 (2009) 141–150, https://doi.org/10.1016/j.canlet.2009.05.004.
[74] C. Wang, R. Xiang, X. Zhang, Y. Chen, Doxycycline inhibits leukemic cell migration via inhibition of matrix metalloproteinases and phosphorylation of focal adhesion kinase, Mol. Med. Rep. 12 (2015) 3374–3380, https://doi.org/10.3892/mmr.2015.3833.
[75] F. Aboubakar Nana, M. Lecocq, M.Z. Ladjemi, B. Detry, S. Dupasquier, O. Feron, P. P. Massion, Y. Sibille, C. Pilette, S. Ocak, Therapeutic potential of focal adhesion kinase inhibition in small cell lung cancer, Mol. Cancer Therapeut. 18 (2019) 17–27, https://doi.org/10.1158/1535-7163.MCT-18-0328.
[76] N.N. Mon, S. Ito, T. Senga, M. Hamaguchi, FAK signaling in neoplastic disorders: a linkage between inflammation and cancer, Ann. N. Y. Acad. Sci. 1086 (2006) 199–212, https://doi.org/10.1196/annals.1377.019.